JOURNAL OF INTEGRAL EQUATIONS
AND APPLICATIONS
Volume 25, Number 3, Fall 2013

# RECONSTRUCTION FOR CAVITIES WITH IMPEDANCE BOUNDARY CONDITION

HAI-HUA QIN AND JI-CHUAN LIU

Communicated by Paul Martin

ABSTRACT. In this paper, we consider the inverse scattering problem of recovering the shape of a cavity or the surface impedance from one source and a knowledge of measurements placed on a curve inside the cavity. Based on a potential approach the inverse problem is equivalent to a system of nonlinear and ill-posed integral equations, a regularized Newton iterative approach is applied to reconstruct the boundary and the injectivity for the linearized system is established. Numerical examples are provided showing the viability of our method.

**1. Introduction.** In some industrial applications of non-destructive testing, it is important to monitor the structural integrity of some cavity using acoustic or electromagnetic waves emitted and measured by sources and receivers placed inside the cavity, such as monitoring the structural integrity of the fusion reactor by electromagnetic waves [**15**]; such a problem can be called the *inverse interior scattering problem*. As noted in [**25**], in some ways the interior scattering problem is physically more complicated than the usual exterior scattering problem, since now all the scattered waves are "trapped." To the authors' knowledge, there are only a few papers to solve this kind of inverse interior scattering problem. In [**15**] potential methods and the range test were used to test the structural integrity of the cavity. In [**25, 28**] the linear sampling method (cf. [**8, 10**]) was applied to recover the

2010 AMS *Mathematics subject classification.* Primary 35J25, 45Q05, 65R30, 78A46.

*Keywords and phrases.* Inverse scattering problem, shape of a cavity, surface impedance, potential approach, nonlinear integral equations.

The research of the first author was supported in part by the Tianyuan fund for Mathematics of the NSF of China (11126184) and the Fundamental Research Funds for the Central Universities (2011QNA27). The research of the second author was supported in part by the NSF of China (10971089) and a scholarship from the Postgraduate Scholarship Program of the China Scholarship Council.

Received by the editors on July 29, 2012, and in revised form on December 28, 2012.

DOI:10.1216/JIE-2013-25-3-431 

shape of a perfectly conducting cavity from a knowledge of sources and measurements located inside the cavity and in [**26**] the method was further extended to reconstruct the shape and the impedance. In a recent paper [**24**], nonlinear integral equations were used to recover the shape of a cavity bounded by a perfectly conducting boundary from a knowledge of measurements and a single point source inside the cavity. However, a perfectly conducting boundary condition is unrealistic. Instead, a more realistic boundary condition is the impedance boundary condition which was first used by Leontovich to model radio wave propagation over the earth [**3**]. In this paper, we consider the scattering of an electromagnetic time-harmonic point source located inside an imperfectly conducting infinite cylinder with bounded cross section $D \subset \mathbf{R}^2$, which is modeled by an interior impedance boundary value problem for the Helmholtz equation inside $D$. The inverse problem we are concerned with is to determine the shape of the boundary $\partial D$ or the impedance function $\lambda$ from a knowledge of the measured scattered fields and a single point source located on a curve $C$ inside $D$.

In this paper, we use a nonlinear integral equation method to solve our inverse problem. The nonlinear integral equation method was first suggested by Kress and Rundell [**19**] where the authors solved an inverse Dirichlet problem for the Laplace equation. Then this kind of method was intensively studied in [**5–7, 12–14, 16, 21, 24, 27**] for the inverse problem in corrosion detection, exterior scattering problems and the shape reconstruction for the perfectly conducting cavity. In this work, we will apply this kind of method to solve our inverse problem, that is, based on a single-layer potential with a density on $\partial D$, we transform our inverse problem into a system of nonlinear and ill-posed integral equations and then solve it by using regularized iterations. The basic idea of the single-layer potential approach came from Cakoni and Kress [**5**] where the authors solved an inverse shape problem in corrosion detection. Finally, we will present some numerical experiments to verify the effectiveness of the method.

The paper is organized as follows. In the next section, we formulate the inverse interior scattering problem mathematically, derive a system of integral equations, prove its equivalence to our inverse shape problem and determine the impedance function for a fixed domain $D$. In Section 3, we give three iteration schemes to reconstruct the boundary and show the injectivity of the linearized system at the exact solution.

Finally, we conclude our paper by providing some numerical examples to show the viability of the proposed methods.

**2. The formulation of the problem.** We now consider the scattering problem of an electromagnetic time harmonic point source located inside an imperfectly conducting infinite cylinder, assuming that a simply connected bounded domain $D \subset \mathbf{R}^2$ with $C^2$ boundary $\partial D$ is the cross section of the infinite cylinder and the electric field is polarized in the TM mode. Then the scattering inside the cylinder is modeled by the following interior impedance boundary value problem

$$\Delta u^s + k^2 u^s = 0 \quad \text{in } D, \tag{2.1}$$

$$\frac{\partial u^s}{\partial \nu} + i\lambda u^s = -\frac{\partial \Phi(\cdot, d)}{\partial \nu} - i\lambda \Phi(\cdot, d) \quad \text{on } \partial D, \tag{2.2}$$

i.e., the total field $u = u^s + \Phi(\cdot, d)$ satisfies

$$\frac{\partial u}{\partial \nu} + i\lambda u = 0 \quad \text{on } \partial D, \tag{2.3}$$

where $k > 0$ is the wave number, $d \in D$ is a fixed point, $\lambda = \lambda(x)$ is a real valued, positive and continuous function defined on $\partial D$, $\nu$ is the unit outward normal to the boundary $\partial D$ and $\Phi$ is the fundamental solution to the Helmholtz equation defined by

$$\Phi(x, d) = \frac{i}{4} H_0^{(1)}(k|x - d|)$$

with $H_0^{(1)}$ being a Hankel function of the first kind of order zero. It is well known that there exists a unique solution $u^s \in H^1(D)$ for $\Phi(\cdot, d) \in H^{1/2}(\partial D)$ to this direct interior impedance boundary value problem (cf. [**4**]).

Now let $C \subset D$ be a closed smooth curve and assume that, for a fixed $d \in C$, we know

$$u^s|_C := u^s(x, d), \quad \text{for all } x \in C. \tag{2.4}$$

The *inverse problem* we are interested in is to determine the boundary $\partial D$ or the impedance function $\lambda$ from a knowledge of the measured

data $u^s$ on a curve $C$ inside $D$ for one single point source located on the curve $C$.

In the following, we will derive an equivalent system of integral equations that we employ for the solution of the inverse problem by a single-layer potential approach. Note that one can also use Green's representation approach (cf. [**19**]) to derive a different equivalent system of integral equations for solving our inverse interior problem, but here we only concentrate on discussing the single-layer potential approach. We introduce the single layer potential

$$u^s(x) = \int_{\partial D} \Phi(x,y)\varphi(y)\, ds(y), \quad x \in D, \tag{2.5}$$

with a density $\varphi \in H^{-1/2}(\partial D)$, and define the integral operators $S_0 : H^{-1/2}(\partial D) \to H^{1/2}(C)$, $S : H^{-1/2}(\partial D) \to H^{1/2}(\partial D)$ and $K' : H^{-1/2}(\partial D) \to H^{-1/2}(\partial D)$ by

$$(S_0\varphi)(x) := \int_{\partial D} \Phi(x,y)\varphi(y)\, ds(y), \quad x \in C, \tag{2.6}$$

$$(S\varphi)(x) := \int_{\partial D} \Phi(x,y)\varphi(y)\, ds(y), \quad x \in \partial D \tag{2.7}$$

and

$$(K'\varphi)(x) := \int_{\partial D} \frac{\partial \Phi(x,y)}{\partial \nu(x)}\varphi(y)\, ds(y), \quad x \in \partial D. \tag{2.8}$$

From now on, we assume that $k^2$ is not a Dirichlet eigenvalue for the negative Laplacian in $D$. Then we have the single-layer potential operator defined by (2.5) from $H^{-1/2}(\partial D)$ to $H^1(D)$ is injective and note that the operator $S$ defined by (2.7) is invertible (cf. [**22**]). Now we can state the following theorem:

**Theorem 2.1.** *Let $D \subset \mathbf{R}^2$ be a bounded simply connected domain with $C^2$ boundary $\partial D$, and assume that $k^2$ is not a Dirichlet eigenvalue for the negative Laplacian in $D$. If $\partial D$ is a solution of the inverse shape problem, then there exists $\varphi \in H^{-1/2}(\partial D)$ such that*

$$\frac{1}{2}\varphi + K'\varphi + i\lambda S\varphi = -\left(\frac{\partial}{\partial \nu} + i\lambda\right)\Phi(\cdot,d)\Big|_{\partial D}, \tag{2.9}$$

$$S_0\varphi = u^s(\cdot,d)|_C\,. \tag{2.10}$$

*Conversely, let $\partial D$ and $\varphi \in H^{-1/2}(\partial D)$ solve the system* (2.9)–(2.10). *Then $\partial D$ is a solution of the inverse shape problem.*

*Proof.* If $\partial D$ is a solution of the inverse shape problem, since $k^2$ is not a Dirichlet eigenvalue for the negative Laplacian in $D$, we can represent the scattered field $u^s$ by (2.5) with an unknown density $\varphi \in H^{-1/2}(\partial D)$ requiring that $u^s$ satisfy the conditions (2.2) and (2.4). Then by the jump relations for the single-layer potential, letting $x$ tend to the boundary from inside $D$, we can obtain (2.9). Further, from (2.4) we obtain (2.10).

Conversely, if $\partial D$ and $\varphi \in H^{-1/2}(\partial D)$ solve the system (2.9)–(2.10), we define $u^s$ by (2.5), and then we obtain that $u^s \in H^1(D)$ satisfies the Helmholtz equation (2.1). Furthermore, from (2.9) and (2.10) we also have that $u^s$ satisfies equations (2.2) and (2.4). Hence, $\partial D$ is a solution of the inverse shape problem. □

Since the inverse problem is ill-posed in the sense that the solution does not depend continuously on the given measured data, we need to apply regularization schemes such as the Tikhonov regularization to solve the ill-posed nonlinear integral equations (2.9)–(2.10) for the given measured data. In this case, the $L^2$-norm will be the appropriate norm to measure the data error and discuss the Tikhonov regularization. Hence, for the remainder of the paper we will consider the operators $S : L^2(\partial D) \mapsto L^2(\partial D)$, $S_0 : L^2(\partial D) \mapsto L^2(C)$ and $K' : L^2(\partial D) \mapsto L^2(\partial D)$. Note that $S : L^2(\partial D) \mapsto H^1(\partial D)$ is invertible provided that $k^2$ is not a Dirichlet eigenvalue for the negative Laplacian in $D$ (cf. [**22**)]. In order to apply the Tikhonov regularization technique to solve the severely ill-posed integral equation (2.10), we state the following theorem [**24**].

**Theorem 2.2.** *The operator $S_0$ is compact, injective and has dense range in $L^2(C)$, provided $k^2$ is not a Dirichlet eigenvalue for the negative Laplacian in the interior of $C$.*

For further analysis and, in particular, for the numerical solution, we first need to parameterize the boundary and the involved integral

operators. We assume that

$$\partial D := \{z(t) = (z_1(t), z_2(t)) : t \in [0, 2\pi]\} \tag{2.11}$$

and

$$C := \{\rho(t) = (\rho_1(t), \rho_2(t)) : t \in [0, 2\pi]\}$$

with $2\pi$ periodic $C^2$-smooth functions $z, \rho : \mathbf{R} \mapsto \mathbf{R}^2$ such that $z$, $\rho$ are injective on $[0, 2\pi)$ and satisfy $z'(t) \neq 0$ and $\rho'(t) \neq 0$ for all $t$. Further, for simplicity, we introduce the notation $a^\perp = (a_2, -a_1)$ for any vector $a = (a_1, a_2)$. Set $\psi := |z'|\varphi \circ z$. Then we obtain from (2.6)–(2.8) the parameterized integral operators as follows

$$[\widetilde{S_0}(z, \psi)](t) = \frac{i}{4} \int_0^{2\pi} H_0^{(1)}(k|\rho(t) - z(\tau)|)\psi(\tau)\, d\tau, \tag{2.12}$$

$$[\widetilde{S}(z, \psi)](t) = \frac{i}{4} \int_0^{2\pi} H_0^{(1)}(k|z(t) - z(\tau)|)\psi(\tau)\, d\tau \tag{2.13}$$

and

$$\begin{aligned}[\widetilde{K'}(z, \psi)](t) \\ = -\frac{ik}{4|z'(t)|} \int_0^{2\pi} H_1^{(1)}(k|z(t) - z(\tau)|) \frac{[z'(t)]^\perp \cdot [z(t) - z(\tau)]}{|z(t) - z(\tau)|} \psi(\tau)\, d\tau\end{aligned} \tag{2.14}$$

for $t \in [0, 2\pi]$, $\psi \in L^2[0, 2\pi]$ and $z \in C^2[0, 2\pi]$. Further, we write the measured data $\omega_0(\rho(t)) := u^s(\rho(t), d)$ and

$$\begin{aligned}[\omega(z)](t) := \frac{ik}{4|z'(t)|} H_1^{(1)}(k|z(t) - d|) \frac{[z'(t)]^\perp \cdot [z(t) - d]}{|z(t) - d|} \\ + \frac{\lambda}{4} H_0^{(1)}(k|z(t) - d|).\end{aligned}$$

Then the system (2.9)–(2.10) is transformed to

$$\widetilde{S_0}(z, \psi) = \omega_0, \tag{2.15}$$

$$\widetilde{K'}(z, \psi) + i\lambda \widetilde{S}(z, \psi) = \omega(z), \tag{2.16}$$

where $\widetilde{K'}(z,\psi) = \psi/(2|z'|) + \overline{K'}(z,\psi)$.

Note that the kernel of $\widetilde{S_0}$ is analytic. For the numerical approximation of the latter, the kernels for the operators $\widetilde{S}$ and $\widetilde{K'}$ can be treated as in [**9**, Chapter 3.5].

To this end, we illustrate that, for a fixed domain $D$, the impedance function $\lambda$ can also be determined from the system (2.9)–(2.10). The process is as follows: we first apply Tikhonov regularization to solve the severely ill-posed integral equation (2.10) with the $L^2$ penalty term for the density $\varphi$ on $\partial D$, then we obtain the operators $K'\varphi$ and $S\varphi$. Finally, the impedance function $\lambda = \lambda(x)$ can be reconstructed by solving the equation (2.9) for each point $x \in \partial D$. This idea had been applied to recover the impedance in corrosion detection and the exterior scattering problems (cf., e.g., [**1, 5**]).

In order to obtain a stable solution we can choose some basis functions $\{\phi_n\}$ and write the impedance function $\lambda$ as

$$\lambda(x) = \sum_n c_n \phi_n(x), \quad x \in \partial D. \tag{2.17}$$

Then the coefficients $\{c_n\}$ can be obtained by solving the equation that is obtained by inserting (2.17) into (2.9) in the least squares sense.

In the following numerical computations, we choose the curve $C$ to be a circle whose radius is $r_c = 0.16$ and the point source $d = r_c(-1, 0)$. The synthetic data $u^s$ on the curve $C$ is obtained by solving the direct problem (2.1)–(2.2) using a single-layer potential approach in which the involved integral equation is solved by Nyström's method [**9**]. Furthermore, to avoid an inverse crime we use triple the number of the discretization points in the forward solver than in the inverse solver in which the involved integral operators were discretized by using the trapezoidal rule with 60 equidistant grid points. In our computation, we use the Tikhonov regularization method to solve (2.10), and the regularization parameter is chosen by the L-curve method which was first applied by Lawson and Hanson [**20**], and we use the Matlab code developed by Hansen [**11**] to obtain the regularization parameter. The basis functions $\phi_n$ are chosen as $\phi_n(x(t)) = \exp(int)$, $n = 0, \pm 1, \ldots, \pm N$, $t \in [0, 2\pi]$. In the following two examples, we use the parameter $N = 4$ and show the numerical results for $k = 2$.

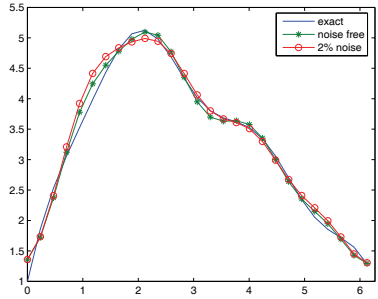


(a) Reconstruction of the impedance for the pear;

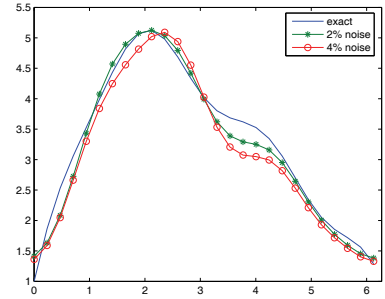


(b) Reconstruction of the impedance for the bean.

FIGURE 1. Reconstruction for the impedance $\lambda$ with $k = 2$.

The first example considered here is a pear parameterized by

$$\partial D = (1.5 - 0.3\cos(3t))\,(\cos t, \sin t)\,, \quad 0 \le t \le 2\pi \tag{2.18}$$

with the parameterized impedance function $\lambda$ given by

$$\lambda(t) = \cos^3 t + \sin t - 0.5t^2 + \pi t. \tag{2.19}$$

The numerical result is shown in Figure 1 (a) for the noiseless case and 2% noisy case.

In the second example we consider a bean parameterized by

$$\partial D = \frac{1 + 0.8\cos t + 0.2\sin(2t)}{1 + 0.7\cos t}\,(\cos t, \sin t)\,, \quad 0 \le t \le 2\pi \tag{2.20}$$

with the impedance function $\lambda$ given by (2.19). The numerical result is shown in Figure 1 (b) with 2% and 4% random noise data.

From Figure 1, we note that the reconstruction method is effective and the numerical result becomes worse when the noise level increases. In order to analyze the sensitivity of the reconstruction with respect

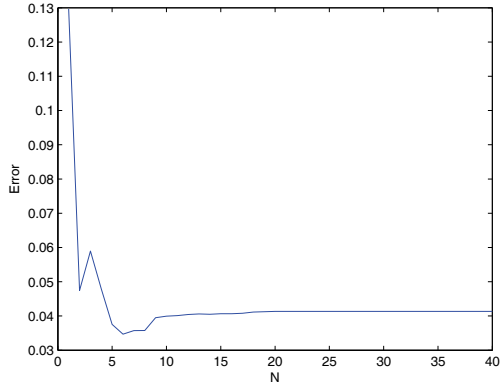


FIGURE 2. Relative error with $k = 2$ and 2% noisy data.

to the parameter $N$, we compute the relative $l^2$ error between the reconstruction $\lambda_{\rm rec}$ and the exact $\lambda$ by

$$\textbf{error} := \left( \sum_{i=1}^{2m+1} |\lambda_{\rm rec}(t_i) - \lambda(t_i)|^2 \right)^{1/2} \Bigg/ \left( \sum_{i=1}^{2m+1} |\lambda(t_i)|^2 \right)^{1/2}, \tag{2.21}$$

where $t_i = (\pi/m)(i-1)$, $i = 1, \ldots, 2m+1$. We display the relationship between **error** and the parameter $N$ for the first example with 2% noisy data in Figure 2. Here, the regularization parameter is obtained again by using the L-curve method. It is shown that the numerical results are stable to the value of the parameter $N$, and we also note that the Tikhonov regularization method with the L-curve technique to solve (2.10) provides an acceptable approximation, while the problem of choosing an optimal regularization parameter needs to be further investigated.

**3. The iteration scheme.** In this section, we will apply three possible iteration techniques for solving the system of integral equations (2.15)–(2.16) for the unknown boundary $\partial D$. In the next section, we will illustrate that these iteration techniques are effective for our inverse interior impedance boundary value problem.

**Method A.** This method is to simultaneously linearize equations (2.15) and (2.16) with respect to $\psi$ and $z$, which was suggested by Kress and Rundell in [**19**] for an inverse boundary value problem for

the Laplace equation and further analyzed in a number of papers [**5, 6, 12, 13, 16, 21, 24**]. Here, the full linearization of (2.15)–(2.16) leads to

$$\widetilde{S_0}(z,\psi)+\widetilde{S_0}(z,\chi)+d\widetilde{S_0}(z,\psi;\zeta)=\omega_0, \tag{3.1}$$

$$\begin{aligned}\widetilde{K'}(z,\psi)+\widetilde{K'}(z,\chi)+d\widetilde{K'}(z,\psi;\zeta)\\ +i\lambda[\widetilde{S}(z,\psi)+\widetilde{S}(z,\chi)+d\widetilde{S}(z,\psi;\zeta)]=\omega(z)+d\omega(z;\zeta).\end{aligned} \tag{3.2}$$

The operators $d\widetilde{S_0}(z,\psi;\zeta)$, $d\widetilde{K'}(z,\psi;\zeta)$, $d\widetilde{S}(z,\psi;\zeta)$ and $d\omega(z;\zeta)$ denote the Fréchet derivatives with respect to $z$ in direction $\zeta$ of the operators $\widetilde{S}_0(z,\psi)$, $\widetilde{K'}(z,\psi)$, $\widetilde{S}(z,\psi)$, and $\omega(z)$, respectively. The Fréchet derivatives of the operators $\widetilde{S}_0$, $\widetilde{K'}$, $\widetilde{S}$ can be obtained by formally differentiating their kernels with respects to $z$ (cf. [**23**]) and $d\omega$ can be obtained by direct differentiation with respect to $z$. Their explicit representations are given by:

$$\begin{aligned}d\widetilde{S_0}(z,\psi;\zeta)(t)&=\frac{ik}{4}\int_0^{2\pi}H_1^{(1)}(k|\rho(t)-z(\tau)|)\frac{[\rho(t)-z(\tau)]\cdot\zeta(\tau)}{|\rho(t)-z(\tau)|}\psi(\tau)\,d\tau,\\ d\widetilde{K'}(z,\psi;\zeta)&=-\frac{z'(t)\cdot\zeta'(t)}{|z'(t)|^2}\widetilde{K'}(z,\psi)-\frac{ik}{4|z'(t)|}\\ &\quad\times\int_0^{2\pi}\left\{\left[kH_0^{(1)}(k|z(t)-z(\tau)|)-\frac{2H_1^{(1)}(k|z(t)-z(\tau)|)}{|z(t)-z(\tau)|}\right]\right.\\ &\quad\times\left.\frac{[z'(t)]^{\perp}\cdot[z(t)-z(\tau)][z(t)-z(\tau)]\cdot[\zeta(t)-\zeta(\tau)]}{|z(t)-z(\tau)|^2}\right\}\psi(\tau)\,d\tau\\ &\quad-\frac{ik}{4|z'(t)|}\int_0^{2\pi}\frac{H_1^{(1)}(k|z(t)-z(\tau)|)}{|z(t)-z(\tau)|}\\ &\quad\times\left\{[\zeta'(t)]^{\perp}\cdot[z(t)-z(\tau)]+[z'(t)]^{\perp}\cdot[\zeta(t)-\zeta(\tau)]\right\}\psi(\tau)\,d\tau,\\ d\widetilde{S}(z,\psi;\zeta)&=-\frac{ik}{4}\int_0^{2\pi}H_1^{(1)}(k|z(t)-z(\tau)|)\\ &\quad\times\frac{[z(t)-z(\tau)]\cdot[\zeta(t)-\zeta(\tau)]}{|z(t)-z(\tau)|}\psi(\tau)\,d\tau\end{aligned}$$

and

$$d\omega(z;\zeta)=\frac{ik}{4|z'(t)|}\left\{-\frac{H_1^{(1)}(k|z(t)-d|)}{|z(t)-d|}\frac{[z'(t)]^{\perp}\cdot[z(t)-d][z'(t)]\cdot[\zeta'(t)]}{|z'(t)|^2}\right.$$

$$+\left[kH_0^{(1)}(k|z(t)-d|)-\frac{2H_1^{(1)}(k|z(t)-d|)}{|z(t)-d|}\right]$$
$$\times\frac{[z'(t)]^\perp\cdot[z(t)-d][z(t)-d]\cdot\zeta(t)}{|z(t)-d|^2}+\frac{H_1^{(1)}(k|z(t)-d|)}{|z(t)-d|}$$
$$\times\left\{[\zeta'(t)]^\perp\cdot[z(t)-d]+[z'(t)]^\perp\cdot\zeta(t)\right\}\Bigg\}$$
$$-\frac{\lambda k}{4}H_1^{(1)}(k|z(t)-d|)\frac{[z(t)-d]\cdot\zeta(t)}{|z(t)-d|}.$$

Note that the kernel for the operator $d\widetilde{S_0}$ is analytic, and the kernel of the second term of $d\widetilde{K'}$ is smooth with its diagonal value given by $-(1/2\pi)[[z'(t)]^\perp\cdot z''(t)z'(t)\cdot\zeta'(t)]/|z'(t)|^4$. The kernel of the third term of $d\widetilde{K'}$ and the kernel of $d\widetilde{S}$ can be treated as in the case of the operator $\widetilde{K'}$.

For a detailed description of the iterative procedure for solving our inverse shape problem via (3.1) and (3.2), we refer to [**19**].

**Method B.** This method is to decompose the inverse problem into a severely ill-posed linear problem and a mildly ill-posed nonlinear problem, which has been studied by Cakoni, Kress, etc., (cf. [**5, 12, 14, 24**]). In this case, we only linearize equation (2.16) with respect to $z$ and obtain the linearized equation

(3.3)
$$\widetilde{K'}(z,\psi)+d\widetilde{K'}(z,\psi;\zeta)+i\lambda[\widetilde{S}(z,\psi)+d\widetilde{S}(z,\psi;\zeta)]=\omega(z)+d\omega(z;\zeta).$$

Then, we can solve our inverse shape problem via (2.15) and (3.3) by an iteration scheme. For the detailed description of the iterative procedure, we refer to [**5**].

**Method C.** This method is for reversing the roles of the equations in Method B, that is, given an approximation $z$ for the boundary, we first solve equation (2.16) for the density $\psi$ and, keeping $\psi$ fixed, linearize (2.15) with respect to $z$ and then solve the linearized equation

$$\widetilde{S_0}(z,\psi)+d\widetilde{S_0}(z,\psi;\zeta)=\omega_0 \tag{3.4}$$

for $\zeta$ to obtain the boundary update $z+\zeta$. The procedure is repeated until a suitable stopping criterion is satisfied. This method has been suggested by Johansson and Sleeman in [**16**] for the exterior scattering

problem and further investigated in much literature (cf., e.g., [**14**] and the references therein).

In the following, we will show injectivity for the linearized system (3.1)–(3.2) at the exact solution. Without loss of generality, we can assume that the perturbation $\zeta$ is in the direction of the normal to the boundary. From now on, we assume that the boundary $\partial D$ is of class $C^3$ to ensure that $\zeta = q[z']^\perp \in C^2[0, 2\pi]$ for a scalar $q \in C^2[0, 2\pi]$ and that the exact solution $u^s$ is twice continuously differential on $\partial D$.

Now, for $\psi \in H^1[0, 2\pi]$ and $\zeta \in C^2[0, 2\pi]$ we define

(3.5)
$$V(x) := -\int_0^{2\pi} \operatorname{grad}_x \Phi(x, z(\tau)) \cdot \zeta(\tau)\psi(\tau) d\tau, \quad x \in \mathbf{R}^2 \backslash \partial D$$

and

(3.6)
$$U(x) := \int_0^{2\pi} \Phi(x, z(\tau))\psi(\tau)\, d\tau, \quad x \in D.$$

Then we have the following lemma.

**Lemma 3.1.** *For $\zeta = q[z']^\perp \in C^2[0, 2\pi]$ with a scalar $q \in C^2[0, 2\pi]$ and $\psi \in H^1[0, 2\pi]$, we have that*

$$\begin{aligned} d\widetilde{K'}(z, \psi; \zeta) = {} & \kappa |z'| q\, (\operatorname{grad} U \cdot \nu) \circ z - k^2 |z'| q U \circ z \\ & - \frac{1}{|z'|} \frac{d}{dt} \left( q \frac{d}{dt} (U \circ z) \right) + (\operatorname{grad} V \cdot \nu) \circ z, \end{aligned}$$

*where $\kappa = [z'' \cdot [z']^\perp]/|z'|^3$ denotes the curvature of the boundary $\partial D$.*

*Proof.* Since

$$\operatorname{grad}_x \frac{\partial}{\partial \nu(y)} \Phi(x, y) = k^2 \Phi(x, y) \nu(y) - \left[ \frac{\partial}{\partial \sigma(y)} \operatorname{grad}_x \Phi(x, y) \right]^\perp,$$
$$y \in \partial D, \quad x \in \mathbf{R}^2 \backslash \{y\},$$

where $\nu$ is the outward normal to $\partial D$ and $\sigma$ is the unit tangent vector in counterclockwise orientation (cf., [**17**, Chapter 7.5]). Then, for any vector $a$, we have

$$\begin{aligned}(3.7)\quad &\left[\operatorname{grad}_x\left([z'(\tau)]^\perp\cdot\operatorname{grad}_y\Phi(x,z(\tau))\right)\right]\cdot a\\ &\qquad=k^2\Phi(x,z(\tau))[z'(\tau)]^\perp\cdot a+\left[\frac{d}{d\tau}\operatorname{grad}_x\Phi(x,z(\tau))\right]\cdot a^\perp.\end{aligned}$$

Since

$$(3.8)\quad \int_0^{2\pi}\psi\widetilde{K}(z,\varphi)\,dt=\int_0^{2\pi}|z'|\varphi\widetilde{K'}(z,\psi)\,dt\quad\text{for all }\varphi,\psi\in H^1[0,2\pi],$$

where

$$\begin{aligned}&\widetilde{K}(z,\varphi)(t)\\ &=\frac{\varphi(t)}{2}+\frac{ik}{4}\int_0^{2\pi}H_1^{(1)}(k|z(t)-z(\tau)|)\frac{[z(t)-z(\tau)]\cdot[z'(\tau)]^\perp}{|z(t)-z(\tau)|}\varphi(\tau)\,d\tau.\end{aligned}$$

Then, similar to the proof of Lemma 3.3 in [**7**], we obtain

$$\begin{aligned}(3.9)\quad &\frac{z'\cdot\zeta'}{|z'|}\widetilde{K'}(z,\psi)+|z'|\,d\widetilde{K'}(z,\psi;\zeta)\\ &\qquad=k^2\int_0^{2\pi}\Phi(z(t),z(\tau))[z'(t)]^\perp\cdot[\zeta(\tau)-\zeta(t)]\psi(\tau)\,d\tau\\ &\qquad\quad+\frac{d}{dt}\int_0^{2\pi}\operatorname{grad}_x\Phi(z(t),z(\tau))\cdot\{[\zeta(t)]^\perp-[\zeta(\tau)]^\perp\}\psi(\tau)\,d\tau\end{aligned}$$

and

$$\begin{aligned}(3.10)\quad &\frac{d}{dt}\int_0^{2\pi}\operatorname{grad}_x\Phi(z(t),z(\tau))\cdot[\zeta(\tau)]^\perp\psi(\tau)\,d\tau\\ &\qquad=-|z'(t)|\,(\operatorname{grad}V\cdot\nu)\circ z\\ &\qquad\quad+k^2\int_0^{2\pi}\Phi(z(t),z(\tau))[z'(t)]^\perp\cdot[\zeta(\tau)]\psi(\tau)\,d\tau.\end{aligned}$$

Further, by the jump relations for the derivative of single-layer potentials, letting $x$ tend to the boundary $\partial D$ from inside $D$, noting that $\zeta^\perp=-qz'$, we obtain

$$(3.11)\quad \int_0^{2\pi}\operatorname{grad}_x\Phi(z(t),z(\tau))\cdot[\zeta(t)]^\perp\psi(\tau)\,d\tau=-q(t)\frac{d}{dt}(U\circ z)$$

and

$$\frac{z' \cdot \zeta'}{|z'|} \widetilde{K'}(z, \psi) = -\kappa |z'|^2 q \, (\operatorname{grad} U \cdot \nu) \circ z. \tag{3.12}$$

Finally, combining (3.9)–(3.12), the proof is completed. □

**Lemma 3.2.** *Under the assumptions of Lemma* 3.1*, we have*

$$d\widetilde{S}(z, \psi; \zeta) = V \circ z + |z'| q (\operatorname{grad} U \cdot \nu) \circ z. \tag{3.13}$$

*Proof.* By the jump relations for single-layer potentials, letting $x$ tend to the boundary $\partial D$ from inside $D$, we have

$$\begin{aligned} V \circ z = &-\frac{1}{2} \zeta(t) \cdot \nu(z(t)) \frac{\psi(t)}{|z'(t)|} \\ &+ \frac{ik}{4} \int_0^{2\pi} H_1^{(1)}(k|z(t) - z(\tau)|) \frac{[z(t) - z(\tau)] \cdot \zeta(\tau)}{|z(t) - z(\tau)|} \psi(\tau) \, d\tau \end{aligned} \tag{3.14}$$

and

$$\begin{aligned} (\operatorname{grad} U \cdot \nu) \circ z = &\frac{\psi(t)}{2|z'(t)|} - \frac{ik}{4|z'(t)|} \\ &\times \int_0^{2\pi} H_1^{(1)}(k|z(t) - z(\tau)|) \frac{[z(t) - z(\tau)] \cdot [z'(t)]^{\perp}}{|z(t) - z(\tau)|} \psi(\tau) \, d\tau. \end{aligned} \tag{3.15}$$

Since $\zeta = q[z']^{\perp}$, combining (3.14) and (3.15), we obtain (3.13). □

Now we can state the injectivity result on the linearized system (3.1)–(3.2) at the exact solution.

**Theorem 3.3.** *Assume that $k^2$ is not a Dirichlet eigenvalue for the region bounded by $C$, and let $z$ be the parameterization of the exact boundary $\partial D$. Let $\psi$ solve equations* (2.15)–(2.16) *for a nonnegative $\lambda \in C[0, 2\pi]$ with $\lambda > k$, and let $u^s$ be the single-layer potential with*

*density* $\psi$. *Assume that* $\zeta = q[z']^{\perp} \in C^2[0,2\pi]$ *for a scalar* $q \in C^2[0,2\pi]$ *and* $\chi \in L^2[0,2\pi]$ *satisfy the homogeneous system*

$$\widetilde{S_0}(z,\chi) + d\widetilde{S_0}(z,\psi;\zeta) = 0, \tag{3.16}$$

$$\widetilde{K'}(z,\chi) + d\widetilde{K'}(z,\psi;\zeta) + i\lambda[\widetilde{S}(z,\chi) + d\widetilde{S}(z,\psi;\zeta)] = d\omega(z;\zeta). \tag{3.17}$$

*Then* $\chi = 0$ *and* $\zeta = 0$.

*Proof.* Define

$$W := w + V \tag{3.18}$$

where

$$w(x) := \int_0^{2\pi} \Phi(x, z(\tau))\chi(\tau)\, d\tau, \quad x \in \mathbf{R}^2 \backslash \partial D \tag{3.19}$$

and $V$ was defined by (3.5). From (3.16), we have $W|_C = 0$. Note that $W$ satisfies $\Delta W + k^2 W = 0$ inside $C$ and, since $k^2$ is not a Dirichlet eigenvalue in the interior of the curve $C$, we have that $W = 0$ inside $C$ (cf. [**2**]). By the unique continuation principle we have $W = 0$ in $D$. Then, by the jump relations for single-layer and double-layer potentials, letting $x$ tend to the boundary $\partial D$ from inside $D$, we obtain

$$\begin{aligned}(\operatorname{grad} W \cdot \nu) \circ z + i\lambda(W \circ z) = \widetilde{K'}(z,\chi) + (\operatorname{grad} V \cdot \nu) \circ z \\ + i\lambda(\widetilde{S}(z,\chi) + V \circ z) = 0,\end{aligned} \tag{3.20}$$

where $V \circ z$ is given by (3.14) and $\widetilde{K'}(z,\chi) = \chi/(2|z'|) + \overline{K'}(z,\chi)$. Combining (3.17) and (3.20), we obtain

$$d\widetilde{K'}(z,\psi;\zeta) + i\lambda\, d\widetilde{S}(z,\psi;\zeta) - (\operatorname{grad} V \cdot \nu) \circ z - i\lambda V \circ z = d\omega(z;\zeta). \tag{3.21}$$

Since $u^s$ is the single-layer potential with density $\psi$, recalling the definition of $U$ given by (3.6), we identify $u^s = U$ and note that $u^s$ satisfies the impedance boundary condition due to the fact that $\psi$ solves equations (2.15)–(2.16). Hence, by Lemmas 3.1, 3.2 and (3.21), we have

$$\begin{aligned}(\kappa + i\lambda)|z'|q\,(\operatorname{grad} u^s \cdot \nu) \circ z - k^2|z'|qu^s \circ z \\ - \frac{1}{|z'|}\frac{d}{dt}\left(q\frac{d}{dt}(u^s \circ z)\right) = d\omega(z;\zeta).\end{aligned} \tag{3.22}$$

Further, by the impedance boundary condition (2.2) and (3.22), we have

$$(3.23)\quad (k^2-\lambda^2)|z'|qu^s\circ z+\frac{1}{|z'|}\frac{d}{dt}\left(q\frac{d}{dt}(u^s\circ z)\right)+i\lambda|z'|q\kappa u^s\circ z$$
$$=-\left(d\omega(z;\zeta)+(\kappa+i\lambda)|z'|q\left((\operatorname{grad}\Phi(\cdot,d)\cdot\nu)\circ z+i\lambda\Phi(z,d)\right)\right),$$

and, after computation, we can obtain

$$(3.24)\quad -d\omega(z;\zeta)+k^2|z'|q\Phi(z,d)+\frac{1}{|z'|}\frac{d}{dt}\left(q\frac{d}{dt}\Phi(z,d)\right)$$
$$=(\kappa+i\lambda)|z'|q(\operatorname{grad}\Phi(\cdot,d)\cdot\nu)\circ z.$$

Combining (3.23) and (3.24), we obtain

$$(k^2-\lambda^2)|z'|qu\circ z+\frac{1}{|z'|}\frac{d}{dt}\left(q\frac{d}{dt}(u\circ z)\right)+i\lambda|z'|q\kappa u\circ z=0,$$

where $u=u^s+\Phi(\cdot,d)$. Further, we have

$$(3.25)\quad (k^2-\lambda^2)\zeta\cdot\nu(z)u\circ z+\frac{d}{ds}\left(\zeta\cdot\nu(z)\frac{du}{ds}\circ z\right)+i\lambda\kappa\zeta\cdot\nu(z)u\circ z=0,$$

where $s$ denotes arc length.

Following the idea in [**18**], multiplying (3.25) by the conjugate complex $\overline{u}$ and taking the real part, we obtain

$$(3.26)\quad (k^2-\lambda^2)\zeta\cdot\nu|u|^2+\frac{1}{2}\frac{d}{ds}\left(\zeta\cdot\nu\frac{d|u|^2}{ds}\right)-\zeta\cdot\nu\left|\frac{du}{ds}\right|^2=0\quad\text{on }\partial D.$$

Now, if $\zeta\cdot\nu$ is not identically zero, without loss of generality, one can assume that the set $I=\{x\in\partial D:\zeta\cdot\nu>0\}$ is nonempty. Then, from (3.26), we have

$$(3.27)\qquad \int_I\left\{(k^2-\lambda^2)|u|^2-\left|\frac{du}{ds}\right|^2\right\}\zeta\cdot\nu\,ds=0.$$

Since $\lambda>k$, from (3.27) we obtain $u=0$ on $I$ and then the impedance boundary condition for $u$ implies $\partial u/\partial\nu=0$ on $I$. Then Holmgren's

theorem implies that $u = 0$ in $D\backslash\{d\}$, i.e., $u^s + \Phi(\cdot, d) = 0$ in $D\backslash\{d\}$, and we immediately have the contraction from the fact that $u^s$ is bounded in $D$ but $\Phi(\cdot, d)$ is not. Hence, we conclude that $\zeta \cdot \nu(z) = 0$, i.e., $q[z']^\perp \cdot [z']^\perp = 0$ which means $\zeta = 0$. Now

$$W(x) = \int_0^{2\pi} \Phi(x, z(\tau))\chi(\tau)\, d\tau, \quad x \in \mathbf{R}^2\backslash\partial D.$$

From (3.16), we get $W|_C = 0$. Since $k^2$ is not a Dirichlet eigenvalue in the interior of $C$ and the unique continuation principle yields $W = 0$ in $D$, then $W = 0$ on $\partial D$. Since $\triangle W + k^2 W = 0$ in $\mathbf{R}^2\backslash\overline{D}$ and $W$ satisfies the Sommerfeld radiation condition, then the continuity of the single-layer potential and the uniqueness for the exterior Dirichlet boundary value problem yield $W = 0$ in $\mathbf{R}^2\backslash\overline{D}$. Finally, the jump relation for the gradient of the single-layer potential yields $\chi = 0$. □

**4. Numerical examples.** In this section, we present several numerical examples to illustrate the effectiveness of reconstruction methods as described in the previous section. For simplicity, we assume that the interior curve $C$ is a circle, i.e., $C = \{\rho(t) \mid \rho(t) = r_c(\cos t, \sin t),\ t \in [0, 2\pi]\}$, where $r_c > 0$ is a constant. The synthetic data $u^s$ on curve $C$ is obtained by solving the direct problem (2.1)–(2.2) using a single-layer potential approach in which the involved integral equation is solved by Nyström's method [**9**]. Furthermore, to avoid an inverse crime, we use a different number of collocation points in the forward solver than in the inverse solver. We apply the trapezoidal rule to discretize integral equations occurring in (3.1)–(3.2), (2.15) and (3.3), (2.16) and (3.4) with $M$ equidistant grid points and use the Tikhonov regularization technique to solve them with the $L^2$ penalty term for the density $\psi$, the updates $\chi$ and $\zeta$. Recalling the form $\zeta = q[z']^\perp$ of the boundary perturbation, the magnitude $q$ of the normal perturbation is approximated by a trigonometric polynomial of degree less than or equal to $m \in \mathbf{N}$, i.e.,

$$q(t) \approx \sum_{j=0}^{m} a_j \cos(jt) + \sum_{j=1}^{m} b_j \sin(jt).$$

The corresponding regularization parameters are denoted as $\alpha_\psi$, $\alpha_\chi$ and $\alpha_\zeta$. For the purpose of illustration, the regularization parameters

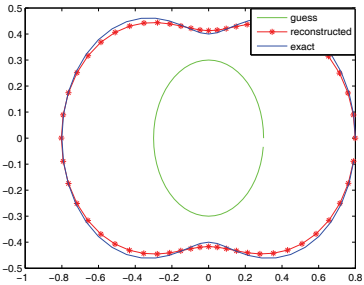


(a) Method A;

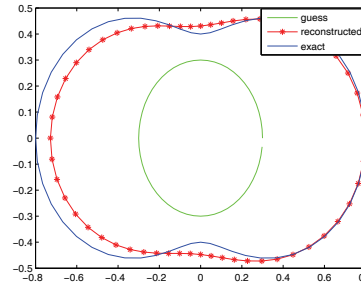


(b) Method B;

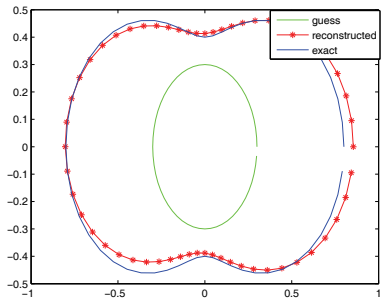


(c) Method C.

FIGURE 3. Reconstruction for $\partial D_p$ with $k = 2$, $\lambda = 4 + \sin^3 t$ and 1% noise.

are chosen by trial and error in the following numerical examples. More research is required on a more sophisticated choice of the regularization parameter to improve the performance. Furthermore, for Methods B and C as observed in [**5, 19**] we need an additional regularization by updating the density $\psi$ by $\psi_{new} = \gamma\psi + (1-\gamma)\psi_{old}$, where $\psi$ is the solution of equations (2.15) and (2.16), respectively, and $\gamma$ is chosen between 0.5 and 0.75.

In the following numerical computations, we always take the source point $d = r_c(-1, 0)$ and the equidistant grid points $M = 56$, choose a circle of radius $r_o$ centered at origin as the initial guess for the boundary to start the iterations and fix the number of iterations to be eight in all the examples.

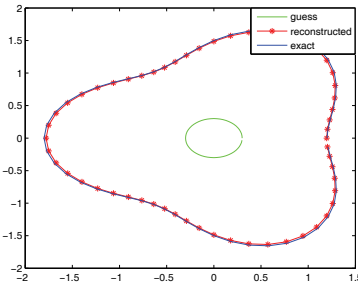


(a) Method A with 1% noise;

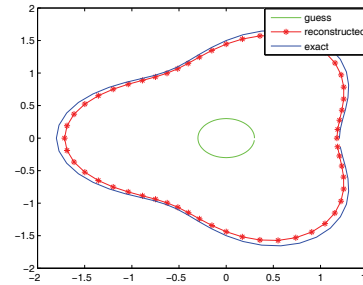


(b) Method A with 5% noise;

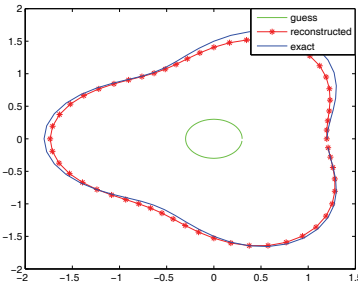


(c) Method B with 1% noise;

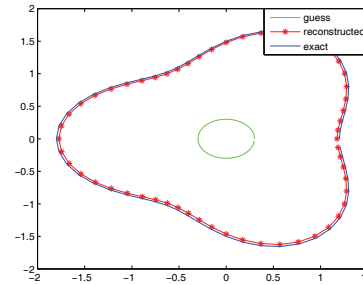


(d) Method C with 1% noise.

FIGURE 4. Reconstruction for $\partial D_a$ with $k = 1$, $\lambda = 4 + \sin^3 t$.

The first example considered here is a peanut parameterized by

$$\partial D_p = 0.8\sqrt{\cos^2 t + 0.25\sin^2 t}\,(\cos t, \sin t)\,, \quad 0 \le t \le 2\pi. \tag{4.1}$$

Reconstructions with $r_c = 0.05$, $r_o = 0.3$, $m = 2$ and $k = 2$ are shown in Figure 3. We display the reconstructions with 1% random noise for $\lambda = 4 + \sin^3 t$. The reconstruction for Method A with $\alpha_\psi = 10^{-9}$ and $\alpha_\chi = \alpha_\zeta = 10^{-6}$ is shown in Figure 3 (a). The reconstruction for Method B is shown in Figure 3 (b) with $\alpha_\psi = 4\times 10^{-10}$ and $\alpha_\zeta = 10^{-7}$, and in Figure 3 (c) we choose $\alpha_\psi = 10^{-13}$ and $\alpha_\zeta = 10^{-7}$ for Method C.

For the second example we consider a pear parameterized by

$$\partial D_a = (1.5 - 0.3\cos(3t))\,(\cos t, \sin t)\,, \quad 0 \le t \le 2\pi. \tag{4.2}$$

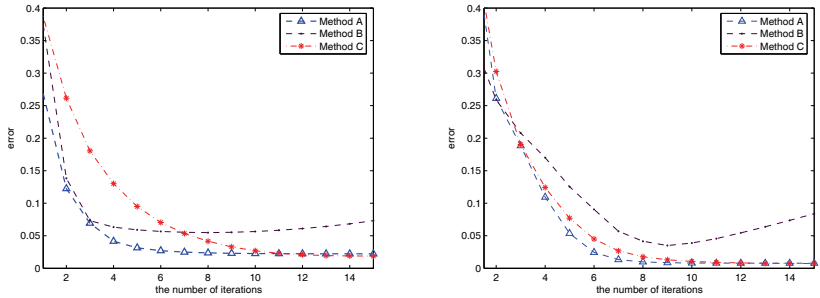


(a) Relative error for the peanut; (b) Relative error for the pear.

FIGURE 5. Relative error for the boundary with $\lambda = 4 + \sin^3 t$ and 1% noise.

The numerical results are shown in Figure 4, where the involved parameters are chosen as $r_c = 0.05$, $r_o = 0.3$, $m = 3$ and $k = 1$. Three methods are also used to recover the shape for $\lambda = 4 + \sin^3 t$. We choose the parameters $\alpha_\psi = 10^{-9}$ and $\alpha_\chi = \alpha_\zeta = 10^{-10}$ in Figure 4 (a) with 1% noise, and $\alpha_\psi = 10^{-10}$, $\alpha_\chi = \alpha_\zeta = 10^{-10}$ in Figure 4 (b) with 5% noise for Method A. In Figure 4 (c), the parameters are chosen as $\alpha_\psi = 10^{-14}$ and $\alpha_\zeta = 10^{-10}$ with 1% noise for Method B, whereas in Figure 4 (d), we choose $\alpha_\psi = \alpha_\zeta = 10^{-10}$ with 1% noise for Method C.

Here we point out that, in our numerical examples, we fix the number of iterations to be eight. In order to analyze the sensitivity of the reconstruction with respect to the number of iterations, recalling the definition of the relative $l^2$ error (2.21), we compute the relative $l^2$ error between the $n$th approximation to the polar radius and the exact polar radius for the peanut $\partial D_p$ and the pear $\partial D_a$, which is a function of the number of iterations, and display the relationship between the relative error and the number of iterations in Figure 5. In Figures 5 (a) and 5 (b), all the parameters are taken to be the same as the first and the second examples, respectively. It is shown that a good approximation can be obtained only with a few iterations, and it seems that Methods A and C are more stable than Method B. Further research is needed in order to obtain a suitable stopping criterion for practical applications.

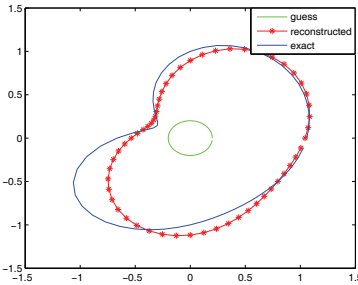


(a) Method A;

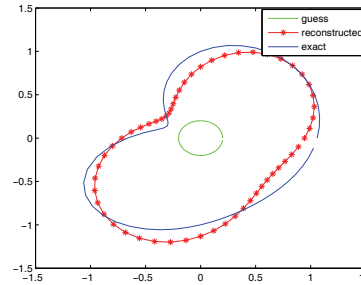


(b) Method B;

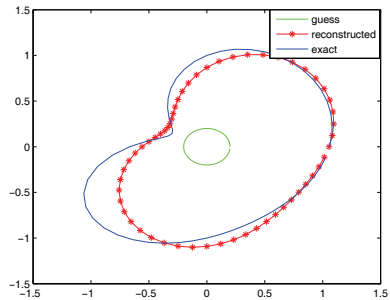


(c) Method C.

FIGURE 6. Reconstruction for $\partial D_b$ with $k = 1$, $\lambda = 5 + \sin^3 t$ and 1% noise.

The third example considered here is a bean parameterized by

$$\partial D_b = \frac{1 + 0.8\cos(t) + 0.2\sin(2t)}{1 + 0.7\cos(t)} (\cos t, \sin t), \quad 0 \le t \le 2\pi. \tag{4.3}$$

The numerical results for $\lambda = 5 + \sin^3 t$ with 1% random noise data are shown in Figure 6, where the choice of the involved parameters is $r_c = 0.02$, $r_o = 0.2$, $m = 2$ and $k = 1$. The reconstruction for Method A with $\alpha_\psi = 10^{-12}$ and $\alpha_\chi = \alpha_\zeta = 10^{-7}$ is shown in Figure 6 (a). The reconstruction for Method B is shown in Figure 6 (b) with $\alpha_\psi = 10^{-12}$ and $\alpha_\zeta = 10^{-10}$, and in Figure 6 (c) we choose $\alpha_\psi = 10^{-10}$ and $\alpha_\zeta = 6 \times 10^{-6}$ for Method C.

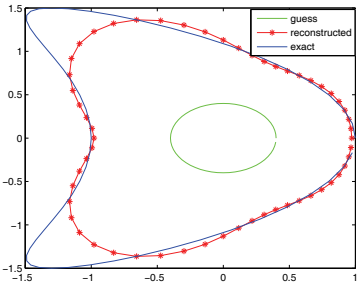


(a) Method A;

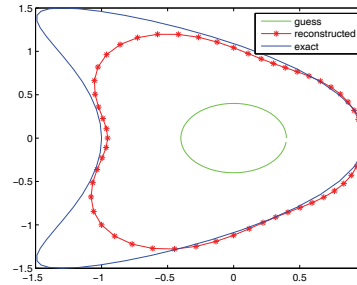


(b) Method B;

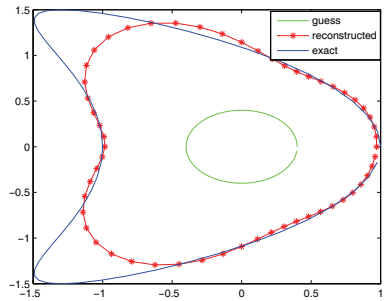


(c) Method C.

FIGURE 7. Reconstruction for $\partial D_k$ with $k = 1$, $\lambda = 5 + \sin^3 t$ and 1% noise.

The fourth example involves the reconstruction of a kite parameterized by

$$\partial D_k = (\cos t + 0.65\cos(2t) - 0.65, 1.5\sin t), \quad 0 \le t \le 2\pi.$$

The numerical results for $\lambda = 5 + \sin^3 t$ with 1% random noise data are shown in Figure 7, where the choice of the involved parameters is $r_c = 0.1$, $r_o = 0.4$, $m = 4$ and $k = 1$. In Figure 7 (a) the parameter is chosen as $\alpha_\psi = 10^{-8}$ and $\alpha_\chi = \alpha_\zeta = 10^{-10}$. In Figure 7 (b), we choose $\alpha_\psi = 10^{-16}$ and $\alpha_\zeta = 10^{-7}$, and we choose $\alpha_\psi = 10^{-10}$ and $\alpha_\zeta = 10^{-8}$ in Figure 7 (c).

From the present numerical examples, we can summarize that the proposed reconstruction approaches are effective, and we can obtain a good

approximation with only a few iterations. From Figures 4 (a)–4 (b) we also note that the reconstruction deteriorates when the noise level increases. In addition, from the present numerical examples, we observe that Method B appears to perform somewhat worse than Methods A and C.

**Acknowledgments.** The authors wish to thank the reviewers' valuable comments and suggestions that have improved our manuscript.

## REFERENCES

**1.** I. Akduman and R. Kress, *Direct and inverse scattering problems for inhomogeneous impedance cylinders of arbitrary shape*, Radio Sci. **38** (2003), 1055–1064.

**2.** T.S. Angell and A. Kirsch, *Optimization methods in electromagnetic radiation*, Springer Mono. Math., Springer-Verlag, New York, 2004.

**3.** L.M. Brekhovskikh, *Waves in layered media*, Appl. Math. Mech. **16**, Academic Press, Inc., New York, 1960.

**4.** F. Cakoni and D. Colton, *Qualitative methods in inverse scattering theory*, in *Interaction of mechanics and mathematics*, Springer-Verlag, Berlin, 2006.

**5.** F. Cakoni and R. Kress, *Integral equations for inverse problems in corrosion detection from partial Cauchy data*, Inverse Prob. Imag. **1** (2007), 229–245.

**6.** F. Cakoni, R. Kress and C. Schuft, *Integral equations for shape and impedance reconstruction in corrosion detection*, Inverse Prob. **26** (2010), 095012, 1–24.

**7.** ———, *Simultaneous reconstruction of shape and impedance in corrosion detection*, Methods Appl. Anal. **17** (2010), 357–378.

**8.** D. Colton and A. Kirsch, *A simple method for solving inverse scattering problems in the resonance region*, Inverse Prob. **12** (1996), 383–393.

**9.** D. Colton and R. Kress, *Inverse acoustic and electromagnetic scattering theory*, Appl. Math. Sci. **93**, Springer-Verlag, Berlin, 1998.

**10.** D. Colton, M. Piana and R. Potthast, *A simple method using Morozov's discrepancy principle for solving inverse scattering problems*, Inverse Prob. **13** (1997), 1477–1493.

**11.** P.C. Hansen, *Regularization tools*: *A Matlab package for analysis and solution of discrete ill-posed problems*, Numer. Algor. **6** (1994), 1–35.

**12.** O. Ivanyshyn and T. Johansson, *Nonlinear integral equation methods for the reconstruction of an acoustically sound-soft obstacle*, J. Int. Equat. Appl. **19** (2007), 289–308.

**13.** O. Ivanyshyn and R. Kress, *Inverse scattering for planar cracks via nonlinear integral equations*, Math. Meth. Appl. Sci. **31** (2008), 1221–1232.

**14.** O. Ivanyshyn, R. Kress and P. Serranho, *Huygens' principle and iterative methods in inverse obstacle scattering*, Adv. Comp. Math. **33** (2010), 413–429.

**15.** P. Jakubik and R. Potthast, *Testing the integrity of some cavity–The Cauchy problem and the range test*, Appl. Numer. Math. **58** (2008), 899–914.

**16.** T. Johansson and B.D. Sleeman, *Reconstruction of an acoustically sound-soft obstacle from one incident field and the far-field pattern*, IMA J. Appl. Math. **72** (2007), 96–112.

**17.** R. Kress, *Linear integral equations*, Appl. Math. Sci. **82**, Springer-Verlag, New York, 1999.

**18.** R. Kress and W. Rundell, *Inverse scattering for shape and impedance*, Inverse Prob. **17** (2001), 1075–1085.

**19.** ———, *Nonlinear integral equations and the iterative solution for an inverse boundary value problem*, Inverse Prob. **21** (2005), 1207–1223.

**20.** C.L. Lawson and R.J. Hanson, *Solving least squares problems*, SIAM, Philadelphia, 1995.

**21.** K.-M. Lee, *Inverse scattering via nonlinear integral equations for a Neumann crack*, Inverse Prob. **22** (2006), 1989–2000.

**22.** W. Mclean, *Strongly elliptic systems and boundary integral equations*, Cambridge University Press, Cambridge, 2000.

**23.** R. Potthast, *Fréchet differentiability of boundary integral operators in inverse acoustic scattering*, Inverse Prob. **10** (1994), 431–447.

**24.** H.-H. Qin and F. Cakoni, *Nonlinear integral equations for shape reconstruction in the inverse interior scattering problem*, Inverse Prob. **27** (2011), 035005, 1–17.

**25.** H.-H. Qin and D. Colton, *The inverse scattering problem for cavities*, Appl. Numer. Math. **62** (2012), 699–708.

**26.** ———, *The inverse scattering problem for cavities with impedance boundary condition*, Adv. Comp. Math. **36** (2012), 157–174.

**27.** P. Serranho, *A hybrid method for inverse scattering for shape and impedance*, Inverse Prob. **22** (2006), 663–680.

**28.** F. Zeng, F. Cakoni and J. Sun, *An inverse electromagnetic scattering problem for a cavity*, Inverse Prob. **27** (2011), 125002, 1–17.

Department of Mathematics, China University of Mining and Technology, Xuzhou, Jiangsu 221116, P.R. China
**Email address: qinhaihua526@163.com**

Department of Mathematics, China University of Mining and Technology, Xuzhou, Jiangsu 221116, P.R. China
**Email address: liujichuan2003@126.com**